GS-13 Petrological and geochemical investigation of the Cinder Lake alkaline intrusive complex, Knee Lake area, east-central Manitoba (part of NTS 53L15)

by R.D. Kressall[1], A.R. Chakhmouradian[1] and C.O. Böhm

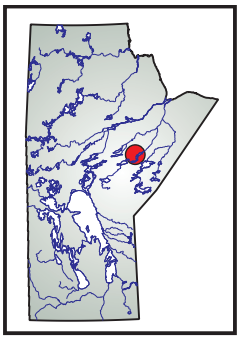

Kressall, R.D., Chakhmouradian, A.R. and Böhm, C.O. 2010: Petrological and geochemical investigation of the Cinder Lake alkaline intrusive complex, Knee Lake area, east-central Manitoba (part of NTS 53L15); *in* Report of Activities 2010, Manitoba Innovation, Energy and Mines, Manitoba Geological Survey, p. 146–158.

Summary

The Cinder Lake alkaline intrusive complex consists of at least four rock types: cancrinite-nepheline syenite, vishnevite syenite, porphyritic cancrinite syenite and alkali-feldspar syenitic pegmatite. New mineralogical, petrographic and geochemical evidence indicates that these rocks form a continuous petrographic series representing either the products of the evolution of a silica-undersaturated alkaline magma or metasomatic reworking of a feldspathoid rock. Abundant evidence of metasomatism at Cinder Lake supports the latter hypothesis. A metasomatic overprint is observed in the feldspathoid syenites, alkali-feldspar syenitic pegmatite and granitoid rocks exposed on some of the islands in Cinder Lake. The source of metasomatic fluids is uncertain, but the abundance of primary calcite in different rocks suggests that these fluids could have emanated from a carbonatite body. Rare earth-element mineralization is observed within the alkaline intrusive rocks at Cinder Lake. Rare earth enrichment appears to be related to metasomatism associated with emplacement of calcite veins, possibly related to the intrusion of a carbonatite body, at Cinder Lake.

The Cinder Lake alkaline rock suite is intrusive into the ca. 2.83–2.71 Ga Knee Lake greenstone belt; however, the relationship between the alkaline and the granitoid rocks of the Bayly Lake complex remains unclear. New zircon and titanite U-Pb isotopic data from a monzogranite sample at Cinder Lake yielded an age of 2721 ±16 Ma. In addition, zircon from a vishnevite syenite sample was dated at 2723 ±10 Ma, whereas titanite from the same sample yielded an age of ca. 2711 ±17 Ma. These age results indicate that both monzogranite and vishnevite syenite were emplaced in the waning stages, or shortly following, the Bayly Lake magmatic event.

Introduction

The Cinder Lake alkaline intrusive complex is to date the only known occurrence of feldspathoid rocks in Manitoba. Despite the extensive geological studies carried out in the surrounding Knee Lake area (i.e., Syme et al., 1997; Syme et al., 1998; Corkery et al., 1999; Corkery et al., 2000), the intrusive rocks at Cinder Lake are not well understood. These rocks include a suite of fine-grained silica-undersaturated syenites and syenitic pegmatites that occur along the lakeshore as a small intrusive body and dikes. The syenites and pegmatites were mapped by Elbers of the Manitoba Geological Survey (MGS) in 1971–1972 as part of the Greenstones project focused on the Gods–Oxford–Knee lakes area (*in* Gilbert, 1985, map). The Cinder Lake area has since been revisited by the MGS (Lenton, 1985) and several exploration companies, but the silica-undersaturated rocks have not been investigated in any detail. The present project was initiated as a joint initiative between the University of Manitoba and the MGS; preliminary results were reported in Chakhmouradian et al. (2008). The present report provides detailed petrographic and geochemical descriptions of the suite of silica-undersaturated syenitic rocks, as well as of granitic rocks exposed at Cinder Lake.

Regional geology

Cinder Lake is located within the Neoarchean Knee Lake greenstone belt (KLGB), which forms part of the Oxford–Stull Terrane (OST) of the Superior Province. The OST marks the boundary between the North Caribou and Northern Superior superterranes (NCS and NSS, respectively). During the formation of the Superior Province, the NCS is interpreted as having acted as the nucleus onto which terranes were accreted from 2.75 to 2.68 Ga, thus including the episode of collision between the NSS and NCS, which occurred around 2.72 to 2.71 Ga and resulted in the imbrication of oceanic crust along the OST (Percival et al., 2006).

The KLGB includes the supracrustal sequences of the Hayes River Group (HRG) and the Oxford Lake Group (OLG; Figure GS-13-1). The HRG is mainly composed of pillow basalt and gabbro with subordinate intermediate and felsic volcanic-sedimentary rocks, which have been dated at 2827–2824 Ma (Corkery et al., 2000). The Bayly Lake plutonic complex consists of tonalitic to granitic plutons that intruded the HRG between 2.78 and 2.73 Ga. The OLG, which consists of a lower 2.72 Ga volcanic subgroup and 2.71 Ga subaerial to shallow-marine sedimentary rocks, is separated from the HRG and Bayly Lake plutonic complex by an unconformity (Corkery et al., 2000).

[1] Department of Geological Sciences, University of Manitoba, 125 Dysart Road, Winnipeg, Manitoba R3T 2N2

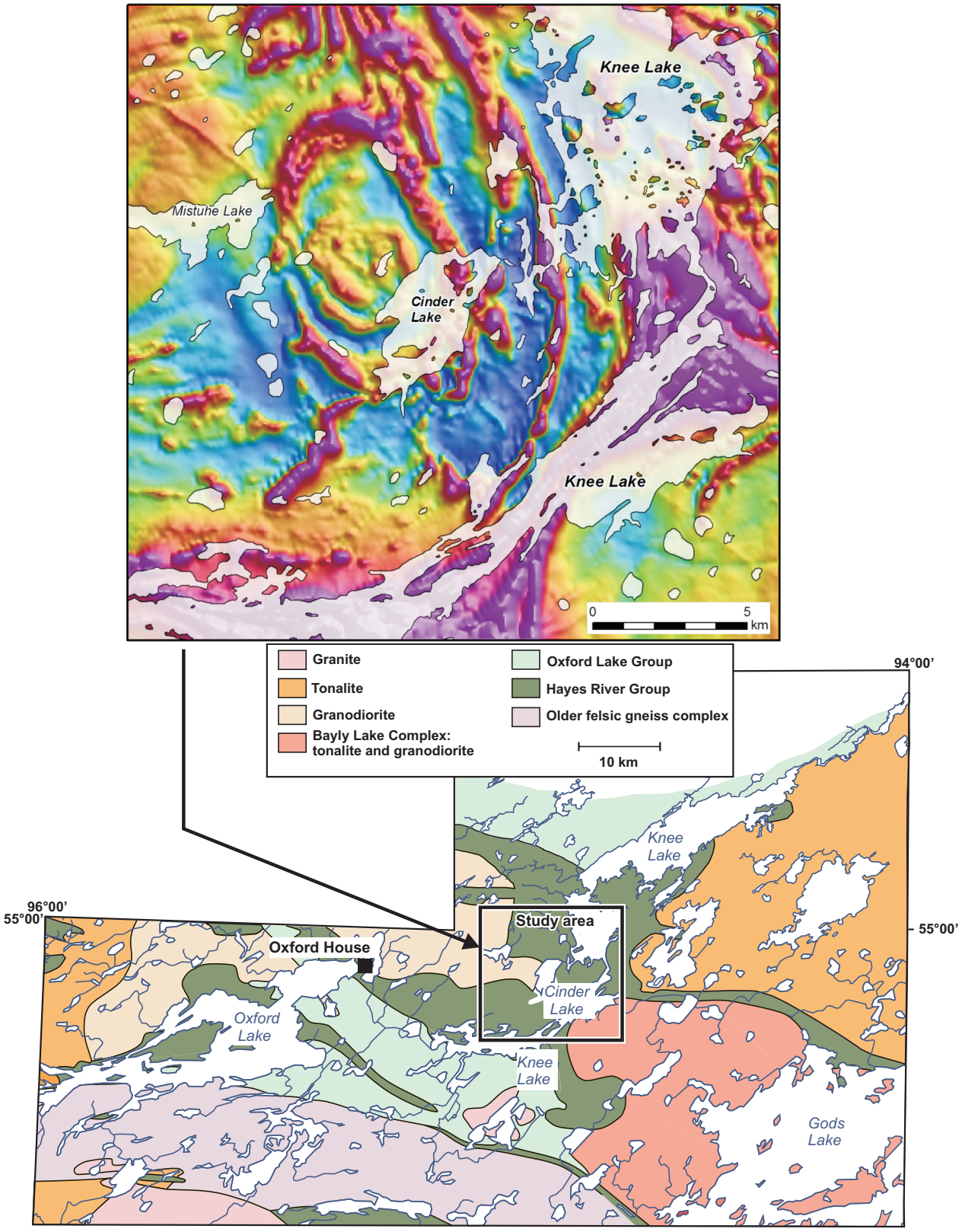

Figure GS-13-1: *Simplified geology of the Knee Lake greenstone belt. Inset shows residual total field map of the Cinder Lake area from the aeromagnetic survey conducted by De Beers Canada (Assessment File 94883, Manitoba Innovation, Energy and Mines).*

Previous mapping included the alkaline rocks as part of the 2.78 and 2.73 Ga Bayly Lake plutonic complex (Gilbert, 1985). However, recent U-Pb dating of a syenite sample from Cinder Lake yielded an age of 2705 ±2 Ma for the alkaline rocks (Chakhmouradian et al., 2008), which is younger than the granitoid rocks included in the Bayly Lake complex and the episode of continental collision between the NSS and NCS, thus placing the alkaline rocks at Cinder Lake in a post-collisional setting.

Methodology

Sampling

Sampling locations are shown in Figure GS-13-2. A first suite of samples was collected by P. Lenton in the summer of 1985; a description of these samples was provided in Chakhmouradian et al. (2008). A second, more extensive set of samples was collected in June 2008. All sampling locations are at or near the shoreline, with the exception of the pegmatite samples and a few samples that were taken from loose rock, where outcrop was not accessible or lacking.

Petrography and mineral chemistry

The petrography of the Cinder Lake samples was studied in polished thin sections using optical microscopy, back-scattered electron (BSE) imaging and Raman spectroscopy at the University of Manitoba. Major-element chemistry of selected minerals was determined by wavelength-dispersive X-ray spectrometry (WDS) at the University of Manitoba using an automated Cameca SX100 electron microprobe operated at 15 kV and 20 nA with an electron beam diameter of 10 µm. Appropriate matrix-specific standards were chosen for each of the analyzed minerals.

Geochemistry

Selected representative samples were sent to Activation Laboratories Ltd.(Ancaster, ON) for sample preparation and whole-rock major- and trace-element analysis. Rock powders were fused with a lithium-metaborate-tetraborate flux and analyzed by inductively coupled plasma–mass spectrometry (ICP-MS).

U-Pb geochronology

Uranium-lead dating of zircon and titanite crystals from vishnevite syenite and monzogranite was conducted

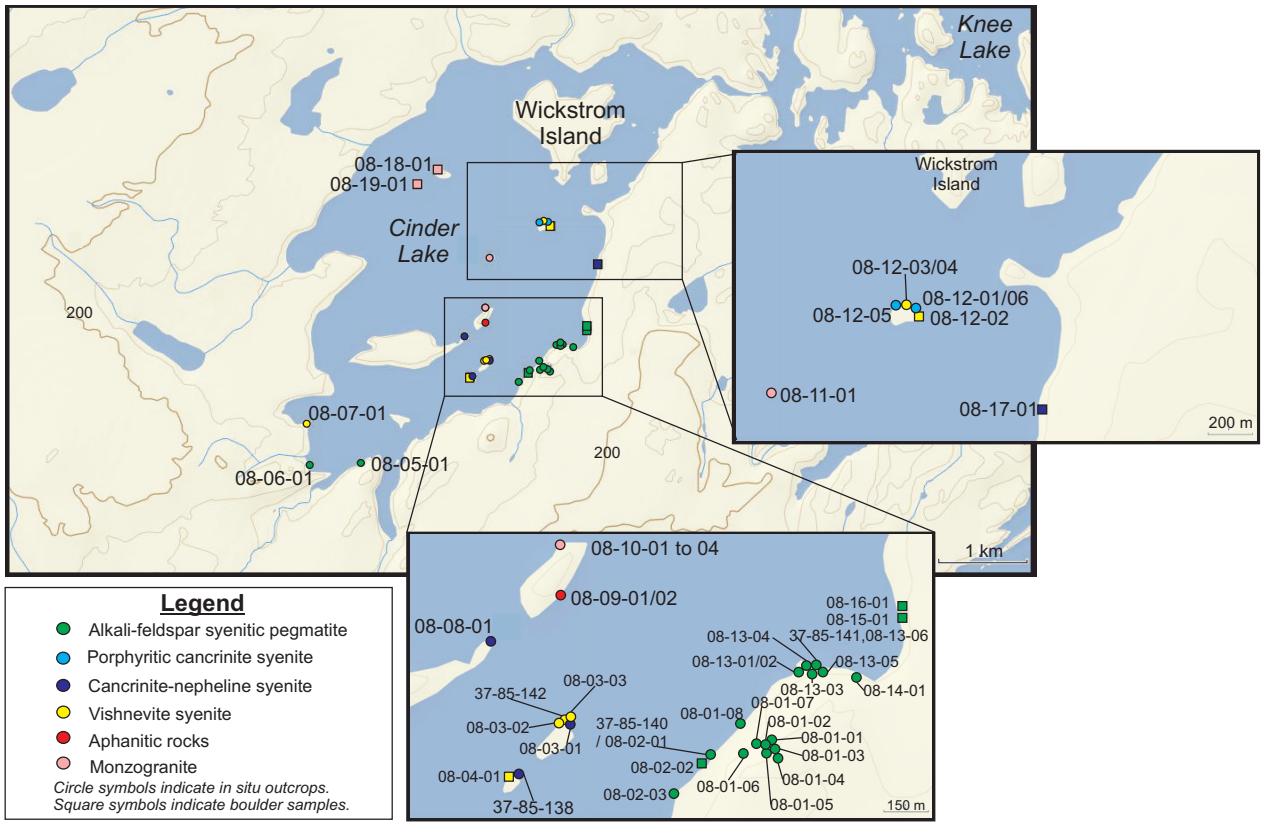

***Figure GS-13-2**: Sample locations at Cinder Lake from 1985 (37-85-#) and 2008 (08-#-#). Locations of 1985 samples are estimated based on field notes. The location of 37-85-139 could not be established and therefore is not shown. Petrographic classification is colour-coded for each sample. Brown lines represent topographic contours in increments of 10 m.*

at the University of Alberta Radiogenic Isotope Facility in Edmonton, Alberta. Approximately 2 kg of massive monzogranite (sample 08-10-01) were crushed and processed using standard mineral separation techniques to obtain zircon and titanite monomineralic separates. The separates were analyzed by isotope dilution–thermal ionization mass spectrometry (ID-TIMS) following the procedures outlined in Heaman et al. (2002). Analyses were performed on a VG354 mass spectrometer, corrected for mass discrimination based on replicate measurement of the NBS981 and U500 standards, and then adjusted for detector bias. Common Pb was calculated using the two-stage model described by Stacey and Kramers (1975).

The U-Pb isotopic compositions of zircon and titanite grains in a thin section of vishnevite syenite (sample 08-12-04) were determined in situ using a Nu Plasma multi-collector–inductively coupled plasma–mass spectrometer (MC-ICP-MS) equipped with a UP-213 laser ablation system. The analytical protocol used for both zircon and titanite was that developed by Simonetti et al. (2006): zircon and titanite analyses were carried out, at a 30 μm beam diameter, using zircon standard LH94-15 and a titanite crystal from the Khan Mine pegmatite, Namibia, respectively. The standards were analyzed at the beginning, the end and approximately in between every 20 point analyses (for zircon) and 16 point analyses (for titanite). Zircon and titanite data were filtered for a high common-Pb content and, in the case of zircon, those analyses with a high ^{204}Pb count were removed from the data. In the case of titanite, the common Pb component was determined by defining a mixing line between the radiogenic Pb component (lower intercept age) and the common Pb component on a Tera-Wasserburg plot (Simonetti et al., 2006). Ages were determined and concordia diagrams plotted using Isoplot version 3.32 in Microsoft Excel (Ludwig, 2005).

Petrography and mineral chemistry of Cinder Lake alkaline intrusive rocks

Cancrinite-nepheline syenite

Cancrinite-nepheline syenite, based on exposures at sampling stations 37-85-138, 08-03-01 and 08-08-01 (Figure GS-13-2), is fine-grained, massive and leucocratic to mesocratic, depending on the relative abundance of mafic minerals. Leucocratic cancrinite-nepheline syenite exposed at station 08-08-01 is devoid of pyroxene. The rock type consists mainly of fine-grained subhedral to anhedral microcline and nepheline partially replaced by albite and cancrinite, respectively (Figure GS-13-3a). The composition of cancrinite (Can) is variable and may contain a significant component of vishnevite (Vsh; $Can_{67-91}Vsh_{9-33}$), a sulphate end-member of the cancrinite group. Other secondary products include muscovite, natrolite and minor stronalsite ($SrNa_2Al_4Si_4O_{16}$), all of which are commonly associated with cancrinite and albite. Stronalsite is a rare Sr-Na feldspar-group mineral found exclusively in silica-undersaturated rocks (e.g., Liferovich and Mitchell, 2006).

Mafic constituents consist of aegirine-augite and phlogopite. Aegirine-augite ($Ae_{40-70}Di_{9-32}Hd_{4-38}$) occurs as euhedral 0.1–1 mm long prisms, although larger grains (1–3 mm) containing a diopside core rimmed by aegirine-augite are locally observed (sample 37-85-138). In addition, andradite commonly forms reaction rims around aegirine-augite. Phlogopite occurs as fine-grained crystals (0.1–0.2 mm) associated with nepheline or cancrinite. Accessory minerals of the cancrinite-nepheline syenite consist of Sr-rich apatite (up to 5.9 wt. % SrO), titanite and magnetite, which is commonly associated with phlogopite. Rare, small (< 50 μm) crystals of monazite and britholite are observed with apatite in some samples.

In contrast to the above-described cancrinite-nepheline syenite, nepheline syenite sampled along the eastern shore of Cinder Lake at station 08-17-01 (Figure GS-13-3b) is devoid of secondary albite or cancrinite (although it does contain rare secondary stronalsite along microcline grain boundaries) and of andradite rims on clinopyroxene. The principal mafic constituent is aegirine-augite overlapping with the compositional range of aegirine-augite from the cancrinite-nepheline syenite ($Ae_{67-81}Di_{9-18}Hd_{9-17}$). Abundant minute inclusions of aegirine (~10 μm) also occur within nepheline. Phlogopite occurs as rare interstitial grains up to 1 mm across associated with aegirine-augite. The nepheline syenite contains a high modal proportion (up to 5 vol. %) of Ca-Na-Zr-Ti silicate tentatively identified here as götzenite, a member of the rosenbuschite mineral group (Figure GS-13-3b). Rosenbuschite-group minerals are complex Ca- and Na-bearing zircono- and titanosilicates that occur as accessory minerals in silica-undersaturated alkaline rocks (e.g., Christiansen and Johnsen, 2003).

Vishnevite syenite

Vishnevite syenite is exposed at sampling stations 37-85-142, 08-03-02, 08-03-03, 08-07-01, 08-12-03 and 08-12-04 (Figure GS-13-2) and is predominant in boulders at 08-12-02. This rock type consists of weakly oriented subhedral to euhedral prisms of microcline, up to 1 mm in length, in a groundmass of vishnevite ($Can_{7-58}Vsh_{42-93}$), albite, calcite and phlogopite (Figure GS-13-3c). Phlogopite is commonly altered to andradite. Accessory minerals consist of titanite, magnetite, Sr-rich apatite, allanite, pyrite, aegirine and zircon. Crystals of Sr-rich apatite (up to 3.1 wt. % SrO) are compositionally zoned with respect to rare earth elements (REE), showing an increase in REE content towards their rim. Allanite occurs commonly along the rim of apatite grains and, less commonly, as aggregates up to 0.2 mm in grain size composed of zoned subhedral prismatic crystals. Rare crystals of aegirine ($Ae_{75-87}Di_{1-4}Hd_{0-4}Jd_{10-19}$) locally occur in association with euhedral pyrite (e.g., sample 08-12-04). Small zircon

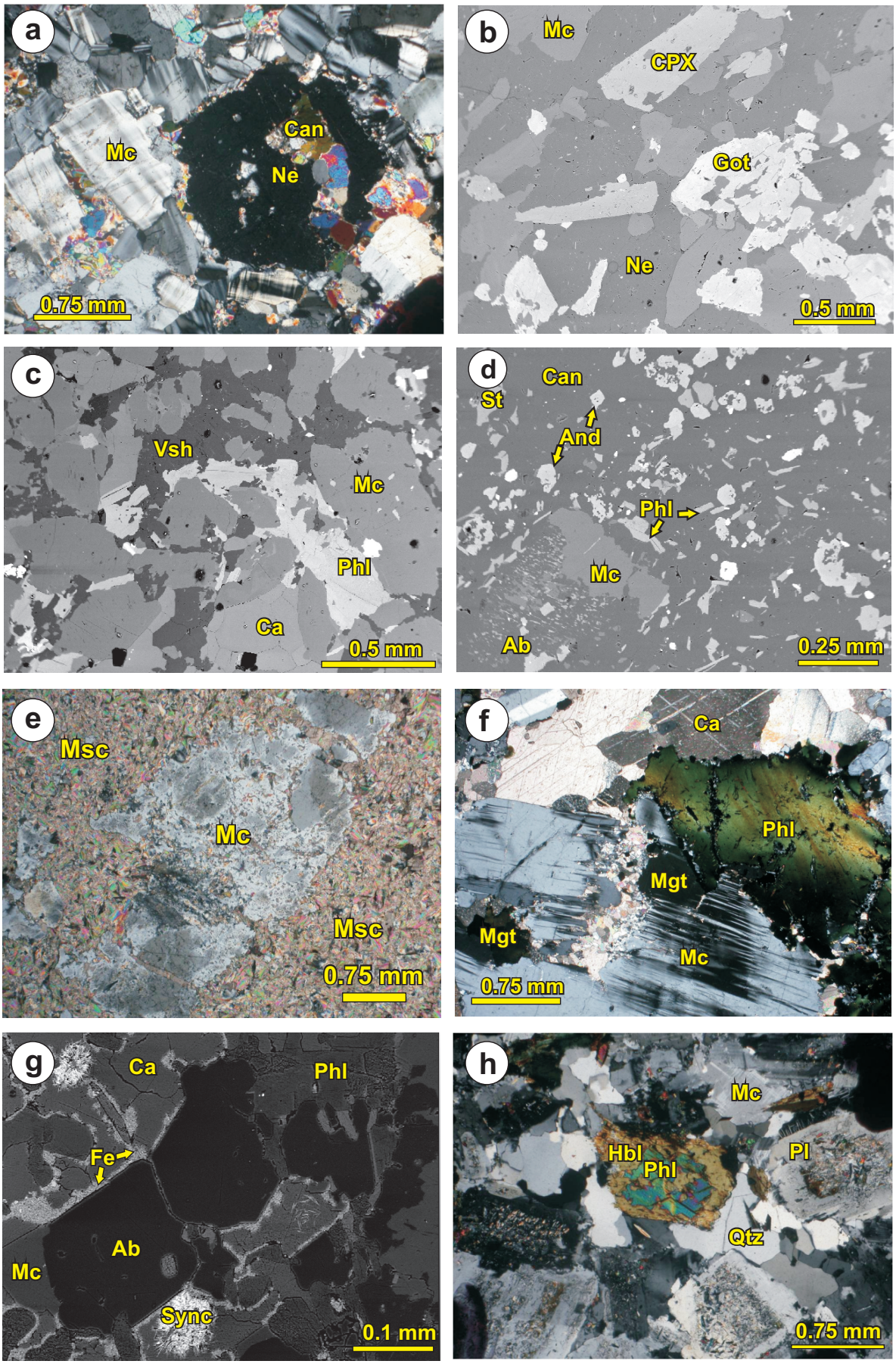
a
Mc
Can
Ne
0.75 mm
b
Mc
CPX
Got
Ne
0.5 mm
c
Vsh
Mc
Phl
Ca
0.5 mm
d
St
Can
And
Phl
Mc
Ab
0.25 mm
e
Msc
Mc
Msc
0.75 mm
f
Ca
Phl
Mgt
Mgt
Mc
0.75 mm
g
Ca
Phl
Fe
Ab
Mc
Sync
0.1 mm
h
Mc
Hbl
Phl
Pl
Qtz
0.75 mm

Previous page: ***Figure GS-13-3****: Petrographic thin-section images of lithological units of the Cinder Lake alkaline intrusive complex:* ***a)*** *nepheline replaced by cancrinite in a matrix of microcline in cancrinite-nepheline syenite (sample 08-08-01), cross-polarized light;* ***b)*** *aegirine-augite and götzenite in a matrix of microcline and nepheline in nepheline syenite (08-17-01), back-scattered electron (BSE) image;* ***c)*** *laths of subhedral microcline in a matrix of vishnevite, calcite and phlogopite in vishnevite syenite (08-03-02). Albite is also typically present within matrix but not visible in image, BSE image;* ***d)*** *alteration of microcline phenocryst to albite+stronalsite in a matrix dominated by cancrinite in porphyritic cancrinite syenite (08-12-05), BSE image;* ***e)*** *albitized microcline in a matrix of muscovite in sericitized alkali-feldspar syenitic pegmatite (08-02-02), cross-polarized light;* ***f)*** *alkali-feldspar syenitic pegmatite with large interstitial phlogopite and calcite veining (08-13-04), cross-polarized light;* ***g)*** *calcite veining in alkali-feldspar syenitic pegmatite with spherulites composed of synchysite and amorphous Fe-oxyhydroxide (08-13-04), BSE image;* ***h)*** *plagioclase and hornblende intergrown with phlogopite in a matrix composed of microcline and quartz in monzogranite (08-10-01). Inclusions within plagioclase consist of epidote, muscovite and titanite, cross-polarized light. Abbreviations: Ab, albite, And, andradite; Ca, calcite; Can, cancrinite; CPX, clinopyroxene; Fe, amorphous Fe-oxihydroxide; Got, götzenite; Mc, microcline; Mgt, magnetite.; Msc, muscovite; Ne, nepheline; Phl, phlogopite; Pl, plagioclase; St, stronalsite; Sync, synchysite; Vsh, vishnevite.*

grains (~50 µm across) are typically present in trace concentrations, except in sample 08-12-04, in which they can reach up to 0.4 mm in diameter.

Boulders sampled at station 08-04-01 are mineralogically similar to the vishnevite syenite, but are characterized by an ocellar-like texture (Figure GS-13-4a). Leucocratic lenses up to 3 cm in length consist of euhedral microcline prisms (with common albite lamellae), up to 4 mm long, set in a mosaic of fine-grained vishnevite and calcite exhibiting triple junctions at grain boundaries (Figure GS-13-4b). The melanocratic phase that hosts the leucocratic lenses is composed of subhedral microcline grains up to 1 mm across in a groundmass dominated by phlogopite with minor vishnevite, calcite and albite

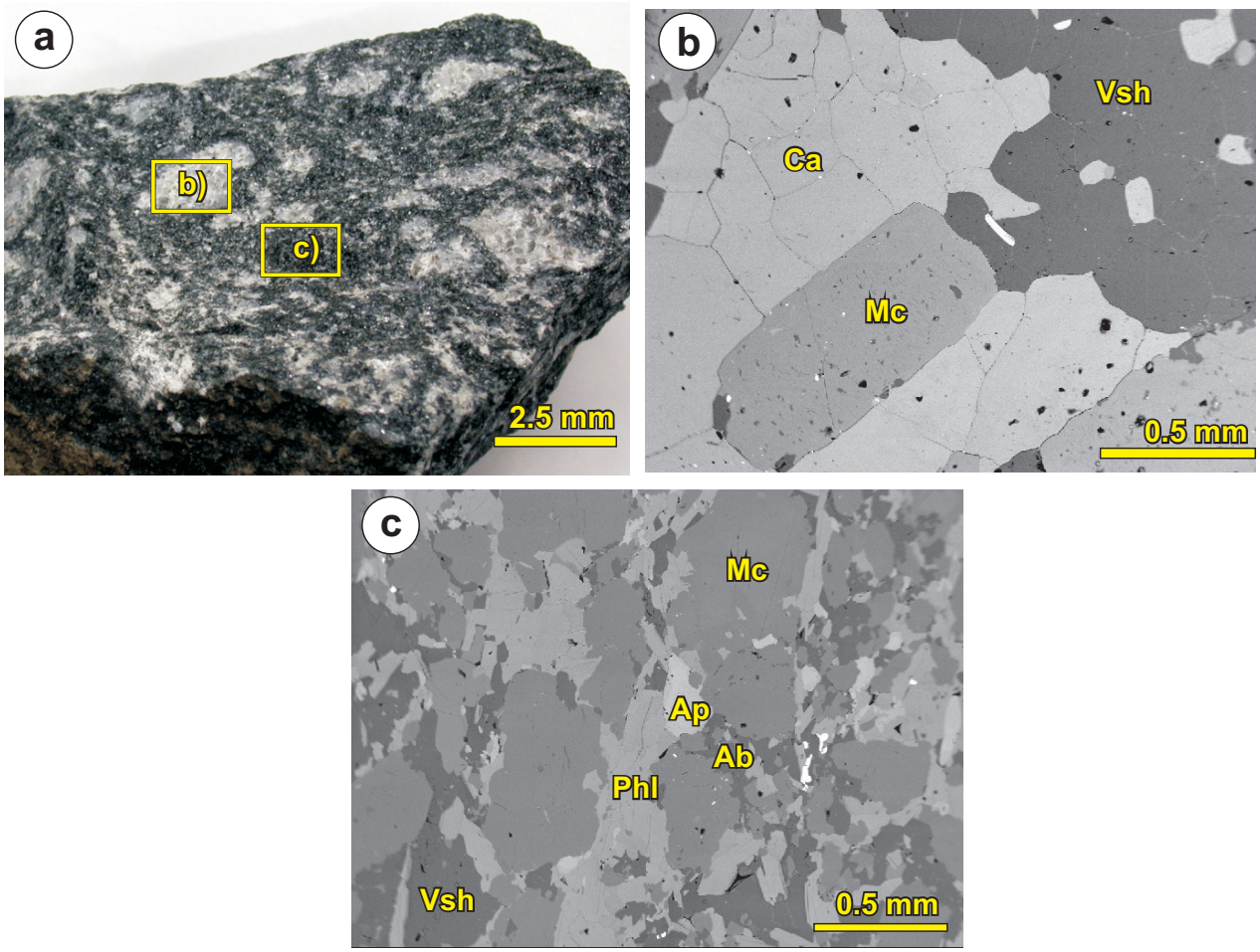

Figure GS-13-4*: Sample from station 08-04-01 at Cinder Lake:* ***a)*** *ocellar-like texture of vishnevite syenite;* ***b)*** *back-scattered electron (BSE) image of leucocratic lenses in ocellar-like vishnevite syenite;* ***c)*** *BSE image of melanocratic phase in ocellar-like vishnevite syenite. Abbreviations: Ab, albite, Ap, apatite; Ca, calcite; Mc, microcline; Phl, phlogopite; Vsh, vishnevite.*

(Figure GS-13-4c). Small (< 50 μm) subhedral allanite and apatite crystals are commonly found as inclusions in phlogopite.

Porphyritic cancrinite syenite

Porphyritic cancrinite syenite outcrops on the island just south of Wickstrom Island at sampling stations 08-12-01/08-12-06 and 08-12-05 (Figure GS-13-2). The unit is composed of dark brown microcline phenocrysts (up to 5 mm in length) set in a fine-grained microcline-albite-cancrinite ($Can_{50-51}Vsh_{49-50}$) groundmass (Figure GS-13-3d), in which the microcline is locally altered to albite and stronalsite. Depending on the degree of microcline alteration, the unit ranges from mesocratic to melanocratic. Whereas microcline constitutes 25 vol. % of the rock in the mesocratic porphyritic cancrinite syenite (sample 08-12-01), it has almost entirely been replaced by albite and stronalsite in the melanocratic porphyritic cancrinite syenite.

Phlogopite is more abundant in the fresher mesocratic porphyritic cancrinite syenite, whereas the more altered melanocratic phase contains abundant andradite (probably developed after phlogopite). Other common accessory minerals include titanite, Sr-rich apatite, fluorite, magnetite, sphalerite, epidote, allanite, calcite, zircon and pyrite.

Alkali-feldspar syenite pegmatite

At the southeastern shore of Cinder Lake, pegmatite forms rocky ridges striking at 45°NE at stations 37-85-139, 37-85-140, 37-85-141, 08-01-01 to -08, 08-02-01, 08-02-03, 08-13-01 to -06 and 08-14-01 (Figure GS-13-2). Pegmatite boulders were sampled at stations 08-02-02, 08-15-01 and 08-16-01, where it appears to have been variably affected by biotitization, albitization, calcitization and sericitization (Figure GS-13-3e). The principal primary constituent of the pegmatite is microcline occurring as dark brown lath-shaped crystals up to several centimetres in length. The volumetric proportions of microcline, albite, calcite and phlogopite are highly variable. Albitization imparts a white to pink colour to the pegmatite, whereas sericitization gives the rock a fine-grained, greenish appearance. Phlogopite and calcite occur commonly as fine-grained veinlets up to 5 cm thick. Medium-grained phlogopite also occurs interstitially between microcline grains in some of the pegmatite samples (Figure GS-13-3f). Euhedral apatite prisms up to 8 mm in length are unevenly distributed throughout the pegmatite, locally composing up to 5 vol. % of the rock.

Calcite veinlets constitute up to 30 % of the pegmatite locally (station 08-13-04, Figure GS-13-3g). Common accessory minerals in the calcite veins include phlogopite, magnetite, fluorite, titanite, rutile, monazite, zircon and spherulites (up to 50 μm in diameter) composed of synchycite and amorphous Fe-oxyhydroxide.

Sericitized alkali-feldspar syenite mineralogically similar to the alkali-feldspar syenitic pegmatite, but much finer grained, occurs at station 08-13-05 in association with pegmatite ridges.

Alkali-feldspar syenitic dikes crosscutting the HRG basalts occur on the southeastern shore of Cinder Lake at stations 08-05-01 and 08-06-01. The dikes consist predominantly of euhedral microcline prisms up to 2.5 cm in length with common albite lamellae. Albitization occurs along microcline grain boundaries and fractures. Accessory euhedral titanite, magnetite, ilmenite, allanite and apatite are common as aggregates up to 1 mm in length. Other common accessory minerals include pyrite, acicular epidote and zircon, with pyrite always occurring with an oxidized rim.

Monzogranite

Monzogranite is exposed on small islands in the western half of Cinder Lake (sampling stations 08-10-01, 08-11-01, 08-18-01 and 08-19-01, Figure GS-13-2). The rock consists of zoned plagioclase prisms (1 to 1.5 mm in size) set in a groundmass of fine-grained anhedral quartz and microcline (Figure GS-13-3h). The composition of the plagioclase crystals ranges from Ab_{78} in the core to Ab_{90-95} in the rim. The plagioclase has undergone partial sericitization and saussuritization to a fine-grained muscovite-epidote aggregate with minor titanite (Figure GS-13-3h). Hornblende constitutes ~5–10 vol. % of the monzogranite; the overall compositional variation of hornblende can be expressed as $(Na_{0.4-0.6}K_{0.1-0.2}Ca_{1.7-1.8})_{\Sigma 2.2-2.6}(Mg_{2.6-2.8}Fe^{2+}_{1.4-1.6}Fe^{3+}_{0.5-0.6}Mn_{0.1}Al_{<0.1})_{\Sigma 5}(Si_{7.1-7.2}Al_{0.8-0.9})_{\Sigma 8}O_{22}(F_{0.4-0.9}OH_{1.1-1.6})_{\Sigma 2}$. Hornblende crystals are commonly zoned to actinolite in the rim: $(Na_{0.1}Ca_{1.9-2.0})_{2.0}(Mg_{3.7-3.8}Fe^{2+}_{0.8-1.1}Fe^{3+}_{0.1-0.3}Mn_{0.1})_5(Si_{7.9}Al_{0.1})_8(F_{0.4}OH_{1.6})_2$. Accessory minerals include phlogopite, titanite and apatite, with phlogopite occurring interstitially and as intergrowths with hornblende.

Fenite

Samples 08-10-02, 08-10-03 and 08-10-04 (Figure GS-13-2) found in the vicinity of the monzogranite have a mineral composition consistent with fenitization of a precursor granitoid; these samples consist of medium-grained microcline, albite, clinopyroxene and, locally, quartz. The composition of clinopyroxene is less sodic in quartz-bearing fenite relative to quartz-free fenite ($Ae_{3-11}Di_{39-62}Hd_{28-48}$ and $Ae_{17-22}Di_{24-29}Hd_{36-46}$, respectively). Accessory minerals consist of pyrite, pentlandite, titanite, zircon, allanite, and andradite (as replacement rims on some quartz grains), with both pyrite and pentlandite showing oxidized rims.

Fine-grained rocks of uncertain affinity

Aphanitic rocks were sampled at stations 08-09-01 and 08-09-02 (Figure GS-13-2). Sample 08-09-01 is light

green and massive, and its mineralogy has not yet been studied. Sample 08-09-02 is light grey and composed of phlogopite, which is commonly altered to andradite, and zoned albite, which ranges in composition from Ab_{91} to Ab_{100}. Accessory minerals consist of titanite, magnetite, pyrite and pentlandite. Pyrite and pentlandite occur as ~25 µm inclusions with oxidized rims within andraditized phlogopite. The rock cannot be reliably classified as either igneous or metasomatic but, based on currently available evidence, it has been classified as 'albitite'; current investigation is in progress.

Geochemistry of Cinder Lake alkaline intrusive rocks

The major-element geochemistry of the rock units described above is plotted in a series of Harker diagrams in Figure GS-13-5. The feldspathoid syenite and alkali-feldspar syenitic pegmatite define a linear trend that involves an increase in Na_2O and Al_2O_3 contents and a decrease in CaO, Fe_2O_3, MgO and P_2O_5 contents with progressively increasing silica levels. The K_2O content is relatively constant in the cancrinite-nepheline syenite and vishnevite syenite (7.3–10.9 wt. %), but is lower in

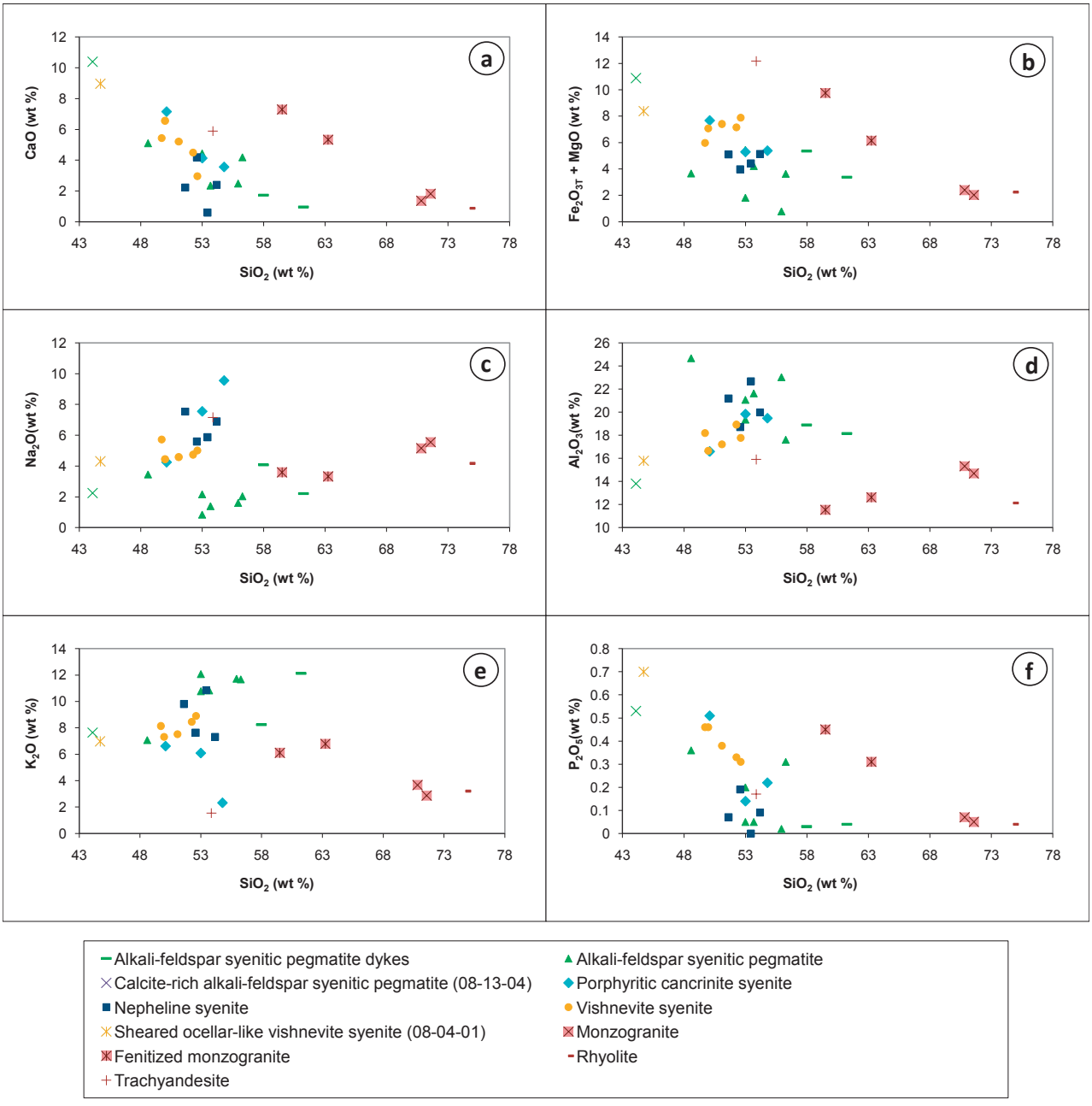

***Figure GS-13-5**: Harker diagrams for selected major-element oxides versus SiO_2: **a)** CaO, **b)** MgO + Fe_2O_3, **c)** Na_2O, **d)** Al_2O_3, **e)** K_2O, **f)** P_2O_5.*

the porphyritic cancrinite syenite (2.3 wt. % in sample 08-12-05), and slightly higher in the alkali-feldspar syenitic pegmatite (10.8–11.7 wt. %, excluding the most metasomatized varieties). The pegmatite has the highest SiO_2 content (53.0–61.2 wt. %, excluding the most metasomatized varieties), followed by cancrinite-nepheline syenite (51.6–54.2 wt. %), porphyritic cancrinite syenite (50.1–53.0 wt. %) and vishnevite syenite (49.7–52.3 wt. %, excluding the ocellar-like variety at station 08-04-01). The pegmatite dikes have a higher SiO_2 content than the pegmatite along the ridge (58.0–61.2 wt. % versus 53.0–56.3 wt. %, respectively). The two most calcite-rich rocks at Cinder Lake, more precisely the ocellar-like vishnevite syenite (sample 08-04-01) and the syenitic pegmatite with abundant calcite veins (sample 08-13-04), have very similar major-element chemistry despite being petrographically different. Both these samples plot at the end of a linear trend with the lowest SiO_2 content. Except for the leucocratic cancrinite-nepheline syenite (sample 08-08-01), all the alkaline rocks examined in this study are metaluminous to mildly peralkaline: $(Na_2O + K_2O)/Al_2O_3$ = 0.85–1.09. The leucocratic cancrinite-nepheline syenite (sample 08-08-01) is marginally peraluminous [Al_2O_3/(Al_2O_3 + CaO + Na_2O) = 1.01].

Another trend is observed in the granitic suite of rocks in Figure GS-13-5. This trend is similar to that observed in the alkaline rocks, except the granitic rocks exhibit a decrease in K_2O content with increasing SiO_2 concentration. Both trends appear to have originated from material characterized by the presence of a low content of SiO_2. The monzogranite has a SiO_2 content of 70.8–71.6 wt. %, whereas the fenite has a much lower SiO_2 content of 59.5–63.24 wt. %. The monzogranite is metaluminous to peraluminous [Al_2O_3/(Al_2O_3 + CaO + Na_2O) = 0.95–1.03], whereas the fenitized rock is peralkaline [($Na_2O + K_2O$)/Al_2O_3 = 1.02–1.08]. The fine-grained rock samples (08-09-01 and 08-09-02) classify as rhyolite and trachyandesite, respectively, in the total alkali versus silica diagram (TAS classification scheme). Sample 08-09-01 (‘rhyolite’) has a similar major-element composition to the monzogranite, but a slightly higher SiO_2 content (74.8 wt. %). The major-element geochemistry of sample 08-09-02 (‘albitite’) does not correlate with the silica-saturated or alkaline series.

Trace-element distributions are shown for selected samples in a spider diagram in Figure GS-13-6. All units show enrichment in large-ion lithophile elements and depletion in high-field-strength elements; notable depletions include Nb, Ta, Ti, Zr and Hf. The monzogranite and porphyritic cancrinite syenite show enrichment in Sr, whereas all the other units show depletion in Sr. Lead is enriched in monzogranite, vishnevite syenite and porphyritic cancrinite syenite, whereas cancrinite-nepheline syenite and alkali-feldspar syenitic pegmatite show depletion in Pb. Thorium and U are enriched in the syenite units, particularly in porphyritic cancrinite syenite. Monzogran-

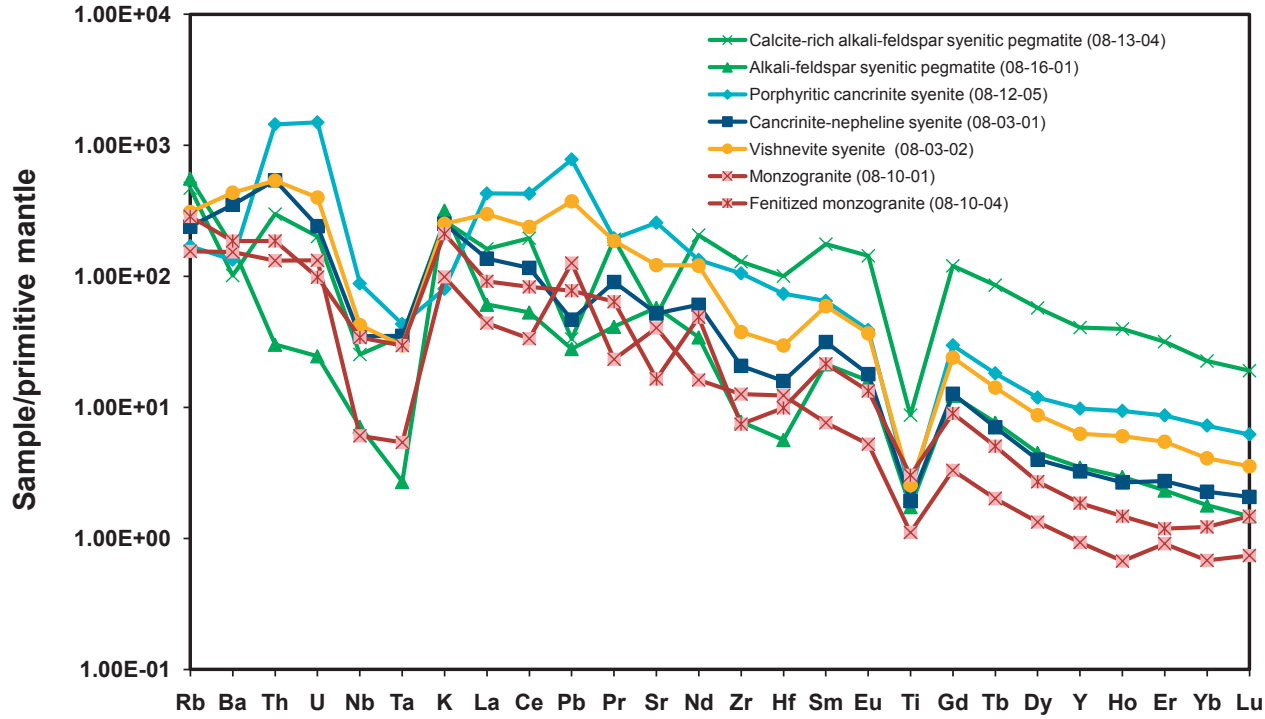

***Figure GS-13-6**: Abundances of selected trace elements for representative samples from Cinder Lake normalized to the primitive mantle of McDonough and Sun (1995).*

ite has the lowest concentration of incompatible trace elements; the fenitized rocks show a similar distribution, but are slightly more enriched in incompatible elements. The syenitic units are more enriched in incompatible trace elements than the granitoid rocks, with porphyritic cancrinite syenite showing the highest enrichment, followed by vishnevite syenite, cancrinite-nepheline syenite and alkali-feldspar syenitic pegmatite. The pegmatite sample with abundant calcite veining (08-13-04) displays a notable enrichment in heavy REE relative to other units at Cinder Lake.

Zircon and titanite U-Pb age results

Age of monzogranite

A few small (0.9 to 2.5 µg) prismatic zircon grains and abundant titanite grains were recovered from monzogranite sample 08-10-01. Four zircon grains and two groups of 20 titanite grains (25.6 and 53.4 mg, respectively) were analyzed by ID-TIMS. The zircon and titanite analyses yielded discordant U-Pb age results shown in Figure GS-13-7. The U-Pb zircon and titanite data were filtered for large errors, which involved removing one zircon (z#2) analysis. Regression of the remaining three zircon analyses results in a lower intercept of 176 ±71 Ma and an upper intercept of 2722 ±12 Ma, while the regression of the two titanite analyses results in a lower intercept of 665 ±190 Ma and an upper intercept of 2744 ±11 Ma. Combined, the three zircon and two titanite analyses yield a lower intercept of 195 ±220 Ma and an upper intercept of 2721 ±16 Ma.

The interpreted age of emplacement of the monzogranite is 2721 ±16 Ma, assuming that the zircon and titanite are magmatic and cogenetic. All three of the above U-Pb ages (zircon, titanite and combined) overlap, within analytical error, with the tail end of Bayly Lake complex magmatism ca. 2.73 Ga, which is consistent with the interpretation that the monzogranite at Cinder Lake is one of the youngest phases of the Bayly Lake complex (Gilbert, 1985).

Age of vishnevite syenite

Nine zircon grains between 50 and 400 µm in diameter were analyzed in thin section using MC-ICP-MS. Between one and 11 point analyses were done on each grain depending on grain size. The data were filtered for common Pb by removing analyses with > 100 cps of ^{204}Pb, and thus reducing the number of analyses from 45 to 13. The remaining 13 analyses yielded discordant U-Pb age data illustrated in Figure GS-13-8. Regression of 13 analyses anchored to a lower intercept of 0 Ma yielded an upper intercept age of 2722 ±10 Ma.

Due to the smaller (50 to 100 µm long) size of titanite grains, only one to five point analyses per grain could be placed into titanite. The titanite analyses were filtered for low ^{206}Pb and high ^{204}Pb counts, reducing the number of analyses from 29 to 17. The remaining 17 analyses are discordant (Figure GS-13-9), yielding an upper intercept age of 2711 ±17 Ma (anchored to 0 Ma).

The 2723 ±10 Ma zircon and 2711 ±17 Ma titanite ages from the vishnevite syenite may suggest ca. 2722 Ma crystallization followed by ca. 2711 Ma tectonothermal overprinting of the vishnevite syenite. In addition, the age data suggest that vishnevite syenite analyzed here is contemporaneous to 2721 ±16 Ma monzogranite but older than 2705 ±2 Ma vishnevite syenite at station 37-85-142 (Chakhmouradian et al., 2008). Alternatively, 2723 ±10 Ma zircons in vishnevite syenite from station

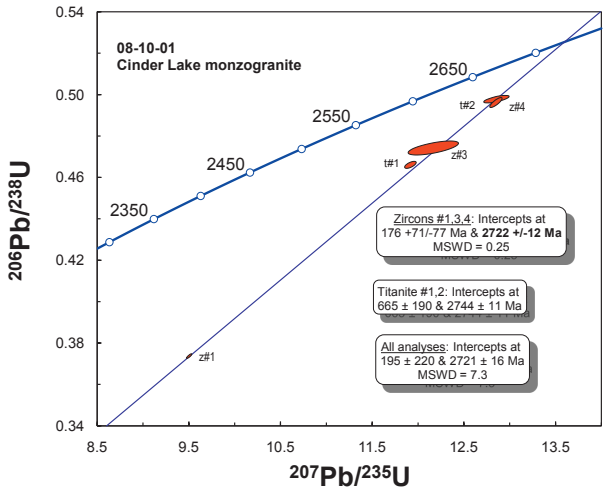

***Figure GS-13-7**: Uranium-lead concordia diagram of zircons (z) and titanite (t) from Cinder Lake monzogranite (sample 08-10-01). Ellipses on concordia diagram are plotted at the 2σ uncertainty level. Abbreviation: MSWD, mean square weighted deviation.*

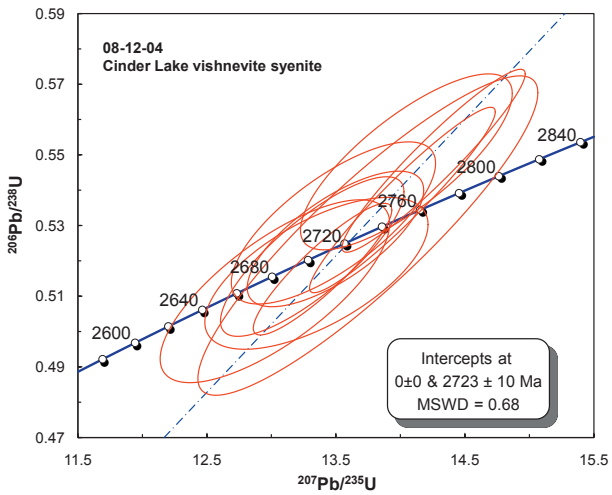

***Figure GS-13-8**: Uranium-lead concordia diagram of zircons from Cinder Lake vishnevite syenite (sample 08-12-04) Ellipses on concordia diagram are plotted at the 2σ uncertainty level. Abbreviation: MSWD, mean square weighted deviation.*

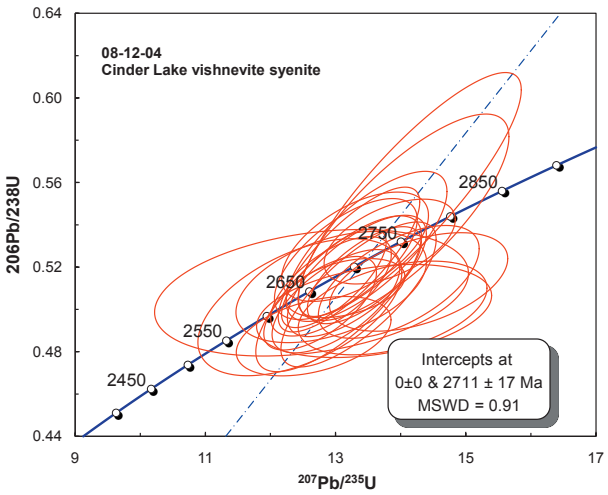

***Figure GS-13-9**: Uranium-lead concordia diagram of titanite from Cinder Lake vishnevite syenite (sample 08-12-04). Ellipses on concordia diagram are plotted at the 2σ uncertainty level. Abbreviation: MSWD, mean square weighted deviation.*

08-12-04 may be inherited from rocks such as the 2721 ±16 Ma monzogranite at Cinder Lake, and the vishnevite syenite is likely ca. 2711–2705 Ma old.

Discussion

The mineralogical and geochemical evidence presented above is consistent with the existence of a single magma-differentiation trend connecting the most primitive rocks (vishnevite syenite) with progressively more evolved ones (porphyritic cancrinite syenite and cancrinite-nepheline syenite) and culminating with the crystallization of the syenitic pegmatite. Alternatively, the low-SiO_2 members of the series (vishnevite syenite and porphyritic cancrinite syenite) may be metasomatic in origin. These two units have a high concentration of deuteric minerals, including members of the cancrinite-vishnevite group, albite, andradite, stronalsite and calcite. The vishnevite syenite has the highest abundance of calcite of all feldspathoid syenites, which is the primary reason for its low SiO_2 content. Although calcite is a common constituent of nepheline syenite elsewhere in the world (Fall et al., 2007; Eby, 2004), it typically occurs as a late-precipitating phase and should not be expected to concentrate in early products of magma differentiation. The intermediate members of the cancrinite-vishnevite series in the syenite units follow the whole-rock trend fairly well. The cancrinite-replacing nepheline contains the lowest vishnevite component, whereas the lowest cancrinite component is observed in the ocellar-like vishnevite syenite. This progression may indicate metasomatism of nepheline syenite by a carbonate-sulphate fluid eventually leading to the formation of vishnevite syenite. The nepheline syenite sample devoid of albite, cancrinite and andradite (08-17-01) may represent the unaltered precursor rock. Its structural relations with cancrinite-nepheline syenite could not be established in the field due to lack of exposure.

The alkali-feldspar syenitic pegmatite and monzogranite show geochemical trends similar to those observed in the fine-grained syenite. The least altered pegmatites have the highest SiO_2 concentrations (i.e., the pegmatite dikes on the southeastern shore of Cinder Lake), while those affected by biotitization, calcitization, albitization and sericitization are similar in composition to the cancrinite-nepheline syenite and vishnevite syenite. For example, sericitized pegmatite sample 08-02-02 is geochemically more similar to the vishnevite syenite than to the other pegmatite samples, despite the obvious differences in mineralogy between these rocks. Similar trends are observed in trace-element distribution patterns and involve a general increase in the content of incompatible elements (particularly, REE) in the porphyritic cancrinite syenite and vishnevite syenite relative to the cancrinite-nepheline syenite (Figure GS-13-6).

An unquestionably metasomatic evolutionary trend is delineated by the monzogranite and fenite compositions in the Harker diagrams (Figure GS-13-5). Interestingly, this fenitization trend appears to have a low-SiO_2 end-member similar to that identified in the alkaline series (see above). This hypothetical low-SiO_2 end-member is the likely source of metasomatism resulting in the observed increase in K_2O, CaO, Fe_2O_3, MgO and P_2O_5 with decreasing SiO_2. It should be noted that, if the alkaline rocks represent a magma-differentiation trend, the alkaline magmas represent the most likely source of fenitization.

A carbonatitic source for the metasomatism is supported by the high content of calcite in the SiO_2-poor members of the alkaline series. The presence of a carbonatite body at Cinder Lake was postulated by Chakhmouradian et al. (2008) based on the presence of Sr-rich calcite, REE-bearing phosphates and Ti-rich andradite veining in the pegmatite.

Based on its U-Pb age of 2721 ±16 Ma, the monzogranite is likely a late-emplaced member of the Bayly Lake suite (2.78 to 2.73 Ga). On the discrimination diagrams of Pearce et al. (1984), the Cinder Lake monzogranite plots within the volcanic-arc granite field, which is consistent with the emplacement of the Bayly Lake complex along an active continental margin during the collision of the NSS with the NCS (Lin et al., 2006). The geochemical similarity between the monzogranite and rhyolite (sample 08-09-01) indicates that these two rock types are probably related, whereas the 'albitite' (sample 08-09-02) cannot be reliably grouped with any other rock type and may simply represent a metasomatized (albitized) member of the HRG suite. Available age data suggests that silica-undersaturated rocks were either replaced at the end of granitic magmatism or may represent a slightly younger suite. The temporal relationship between the monzogranite and the silica-undersaturated rocks at Cinder Lake cannot be distinguished solely based

on geochronological data present in this location; further geochronological work is required to better constrain the relationship between these units. Both the monzogranite and the vishnevite syenite (at station 08-12-04) dated here appear to be older than the vishnevite syenite (at station 37-85-142) dated by Chakhmouradian et al. (2008).

Economic considerations

Mafic volcanic rocks at Cinder Lake have been noted to host massive sulphide mineralization (i.e., Barry, 1959; Assessment File 72612, Manitoba Innovation, Energy and Mines). Barry (1959) noted the occurrence of zones of massive and disseminated sulphide up to 5 m in width on two northernmost islands in Cinder Lake, including Wickstrom Island. Cinder Lake was explored extensively in the 1960s and 1970s for base metals. In the early to mid-1990s Inco Exploration and Technical Services Inc. (Assessment File 72612) intersected several metre-wide intervals of massive and brecciated pyrite and pyrrhotite with sphalerite and chalcopyrite in several drillholes. Appreciable concentrations of Cu and Zn (up to 0.16 and 0.22%, respectively) were assayed by Inco at the time within the massive sulphide zone. De Beers Canada conducted till studies and aerial geophysical surveys in the area in 2000 (Assessment File 94883), including collection of high-resolution aeromagnetic data covering all of Cinder Lake (Figure GS-10-1, inset), to follow up on the discovery of kimberlite indicator minerals in the Knee Lake region (Fedikow et al., 2002).

Of particular interest to current mineral exploration is the abundance of REE minerals in several different rock types at Cinder Lake. A number of REE-bearing minerals have been observed in the fine-grained silica-undersaturated syenite, the metasomatized pegmatite and within calcite veining. The surface sampling by Inco (Assessment File 72612) in the early 1990s yielded five samples with ΣREE_2O_3 concentrations (excluding Gd, Dy, Ho, Er and Tm) greater than 0.10 wt. %, with the highest value exceeding 0.9 wt. %. Inco attributed the REE enrichment to metasomatism associated with the intrusion of alkaline rocks, but did not conduct any follow-up work on their geochemical anomalies. The most likely source of this REE enrichment would be an intrusion or intrusions of carbonatite that are either submerged or too heavily weathered to be recognizable in outcrop. Approximately 80% of all carbonatite localities worldwide are associated with silica-saturated and undersaturated syenite (Woolley, 2003). Based on the aeromagnetic survey performed in 2000, a conservative estimate of the total area occupied by the Cinder Lake alkaline intrusive complex at the current level of erosion is around 25 km^2. This estimate is similar in scale to that of the carbonatite-syenite intrusions at Mountain Pass (California) and Maoniuping (China), both of which host economic REE mineralization. The Mountain Pass orebody (average grade ~8.9 wt % REE_2O_3) was the world's principal source of light REE from the 1960s to the mid-1990s (Castor, 2008). The Maoniuping complex is currently the second largest REE producer in the world, containing over 1.45 million tons of REE_2O_3 in primary and enriched secondary ores ranging in grade from 2.7 to 13.6 wt. % REE_2O_3 (Xu et al., 2004). The geological setting of the Maoniuping and Mountain Pass complexes is similar to that of the Cinder Lake complex, but the former two are related to much younger orogenic events and thus likely better preserved.

Acknowledgments

The authors thank P. Yang and R. Sidhu (University of Manitoba) for their technical support on the electron-microprobe analysis; A. DuFrane (University of Alberta) for his help with in situ thin-section dating; and Canadian International Minerals Inc. for their generous support of this study.

References

Barry, G. S. 1959: Geology of the Oxford House-Knee Lake Area Oxford Lake and Gods Lake Mining Divisions 53L/14 and 53L/15: Manitoba Department of Mines and Natural Resources, Mines Branch, Publication 58-3, 39 p.

Castor, S. B. 2008: Rare earth deposits of North America; Resource Geology, v. 58, p. 337–347.

Chakhmouradian, A.R., Böhm, C.O., Kressall, R.D. and Lenton, P.G. 2008: Evaulation of the age, extent and composition of the Cinder Lake alkaline intrusive complex, Knee Lake area, Manitoba (part of NTS 53L15); *in* Report of Activities 2008, Manitoba Science, Technology, Energy and Mines, Manitoba Geological Survey, p. 109–120.

Corkery, M.T., Lin, S., Bailes, A.H. and Syme, E.C. 1999: Geological investigations in the Gods Lake Narrows area (Parts of NTS 53L/9 and 53 L/10); *in* Report of Activities 1999, Manitoba Industry, Trade and Mines, Geological Services, p. 76–80.

Corkery, M.T., Cameron, H.D., Lin, S., Skulski, T., Whalen, J.B. and Stern, R.A. 2000: Geological investigations in the Knee Lake Belt (parts of NTS 53L); *in* Report of Activities 2000, Manitoba Industry, Trade and Mines, Manitoba Geological Survey, p. 129–136.

Christiansen, C.C. and Johnsen, O. 2003: Crystal chemistry of the rosenbuschite group; The Canadian Mineralogist, v. 41, p. 1203–1224.

Eby, G.N. (2004): Petrology, geochronology, mineralogy and geochemistry of the Beemerville alkaline complex, northern New Jersey; *in* Neoproterozoic, Paleozoic, and Mesozoic Intrusive Rocks of Northern New Jersey and Southeastern New York, J.H. Puffer and R.A.Volkert (ed.), Geological Association of New Jersey, Twenty-First Annual Meeting, Mahwah, New Jersey, 2004, p. 52–68.

Fall, A., Bodnar, R.J., Szabó, C. and Pál-Molnár, E. 2007: Fluid evolution in the nepheline syenites of the Ditrău Alkaline Massif, Transylvania, Romania; Lithos, v. 95, p. 331–345.

Fedikow, M.A.F., Nielsen, E., Conley, G.G., and Lenton, P.G. 2002: Operation Superior: comilation of kimberlite indicator mineral survey results (1996-2001); Manitoba Industry, Trade and Mines, Manitoba Geological Survey, Open File Report OF2002-1, 60 p.

Gilbert, H.P. 1985: Geology of the Knee Lake–Gods Lake area; Manitoba Energy and Mines, Geological Services, Geological Report GR83-1B, 76 p.

Heaman, L.M., Erdmer, P. and Owen, J.V. 2002: U-Pb geochronologic constraints on the crustal evolution of the Long Range Inlier, Newfoundland; Canadian Journal of Earth Sciences, v. 39, p. 845–865.

Lenton, P.G. 1985: GS-40 Granite-pegmatite investigations: Knee Lake–Magill Lake area; *in* Report of Field Activities 1985, Manitoba Energy and Mines, Geological Services, Mine Branch, p. 203–208.

Liferovich, R.P. and Mitchell, R.H. 2006: Paragenesis and composition of banalsite, stronalsite, and their solid solution in nepheline syenite and ultramafic alkaline rocks; The Canadian Mineralogist, v. 44, p. 203–208.

Lin, S., Davis, D.W., Rotenberg, E., Corkery, M.T. and Bailes, A.H. 2006: Geological evolution of the northwestern Superior Province: clues from geology, kinematics, and geochronology in the Gods Lake Narrows area, Oxford–Stull terrane, Manitoba; Canadian Journal of Earth Sciences, v. 43, p. 749–765.

Ludwig, K.R. 2005: Isoplot 3.32: a geochronological toolkit for Microsoft Excel; Berkeley Geochronological Center, Special Publication No. 2, p. 1–22.

McDonough, W.F. and Sun, S.-s. 1995: The composition of the Earth; Chemical Geology, v. 120, p. 223–253.

Pearce, J.A., Harris, B.W.H. and Tindle, A.G. 1984: Trace element discrimination diagrams for the tectonic interpretation of granitic rocks; Journal of Petrology, v. 25, p. 956–983.

Percival, J.A., Sanborn-Barrie, M., Skulski, T., Stott, G.M., Helmstaedt, H. and White, D.J. 2006: Tectonic evolution of the western Superior Province from NATMAP and LITHOPROBE studies; Canadian Journal of Earth Sciences, v. 43, p. 1085–1117.

Simonetti, A.,Heaman, L.M., Chako, T. and Banerjee, N.R. 2006: In situ petrographic thin section U-Pb dating of zircon, monazite and titanite using laser ablation-MC-ICP-MS; International Journal of Mass Spectrometry, v. 253, p. 87–97.

Stacey, J.S. and Kramers, J.D. 1975: Approximation of terrestrial lead isotope evolution by a two-stage model; Earth and Planetary Science Letters, v. 26, p. 207–221.

Syme, E.C., Corkery, M.T., Bailes, A. H., Lin, S., Cameron, H.D.M. and Prouse, D. 1997: Geological investigations in the Knee Lake area, northwestern Superior Province (parts of NTS 53L/15 and 53L/14); *in* Report of Field Activities 1997, Manitoba Science and Mines, Geological Services, p. 37–46.

Syme, E.C., Corkery, M.T., Lin, S., Skulski, T., and Jiang, D. 1998: Geological investigations in the Knee Lake area, northern Superior Province (parts of NTS 53L/15 and 53M/2); *in* Report of Activities 1998, Manitoba Energy and Mines, Geological Services, p. 88–95.

Woolley, A.R. 2003: Igneous silicate rocks associated with carbonatites: their diversity, relative abundances and implications for carbonatite genesis; Periodico di Mineralogia, v. 72, p. 9–17.

Xu, C., Zhang, H., Huang, Z., Liu, C., Qi, L., Li, W. and Guan,T. 2004: Genesis of the carbonatite-syenite complex and REE deposit at Maoniuping, Sichuan Province, China: evidence from Pb isotope geochemistry; Geochemical Journal, v. 38, p. 67–76.